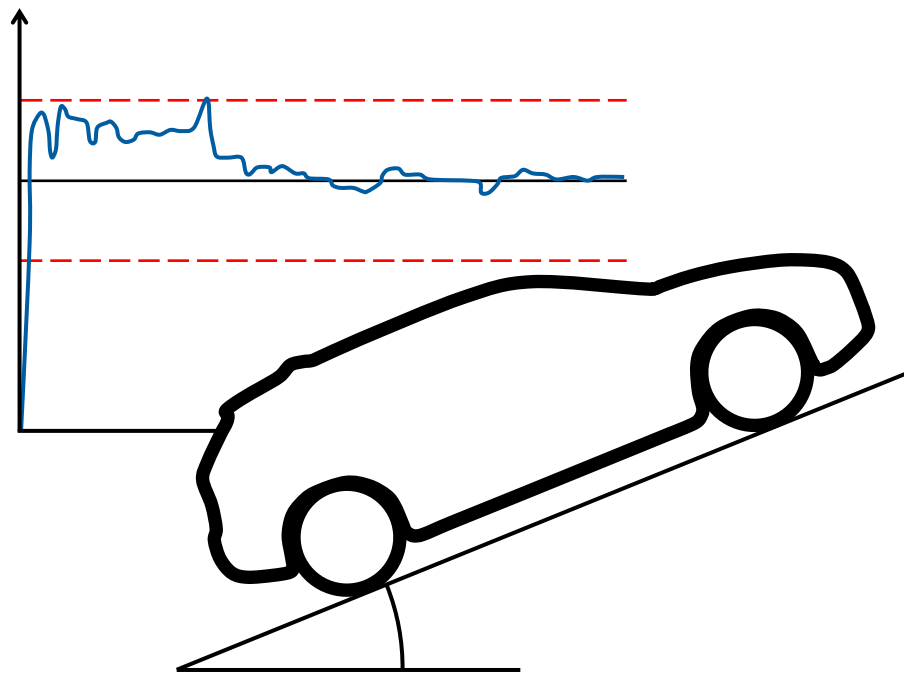


# CHALMERS



## Estimation of Vehicle Mass Using an Extended Kalman Filter

*Master of Science Thesis*

BJÖRN LUNDIN  
ANDRÉAS OLSSON

Department of Signals and Systems  
*Division of Automatic Control, Automation and Mechatronics*  
CHALMERS UNIVERSITY OF TECHNOLOGY  
Gothenburg, Sweden, 2012  
Report No. EX037/2012



## Abstract

Vehicle mass is an important parameter when developing features which improve drivability and performance feel for passenger cars. A vehicle's mass naturally depends on the load and the number of passengers. Therefore it is desired to have a fast, accurate and robust mass estimation algorithm.

In this thesis an extended Kalman filter is used to estimate the mass of a passenger car. The filter uses the wheel torque, vehicle speed and road slope as input, where the road slope is measured by an accelerometer.

The estimation algorithm is tested on real data and in simulated environments. The results show that the filter is fast and sufficiently accurate; it often reaches within 5% of the true mass after a few seconds. However, the results also show how changes in the environmental parameters can reduce the possibilities of getting an accurate estimation.

Keywords: *Extended Kalman filter, mass estimation, road slope estimation, accelerometer, vehicle dynamics, nonlinear system*



## Acknowledgements

We would like to thank Johan Backmark, our supervisor at Volvo Car Corporation, for helping us throughout the project. We would also like to thank the other helpful employees at VCC, especially Anders Brandt and Fredrik Höök. Finally we would like to thank Jonas Fredriksson, our examiner and supervisor at Chalmers University of Technology.

Björn Lundin and Andréas Olsson, Gothenburg, June 2012



# Contents

<b>1</b>	<b>Introduction</b>	<b>1</b>
1.1	Related work . . . . .	1
1.2	Purpose . . . . .	2
1.3	Objectives . . . . .	2
1.4	Method . . . . .	3
1.5	Delimitations . . . . .	3
1.6	Report outline . . . . .	3
<b>2</b>	<b>Background theory</b>	<b>5</b>
2.1	Vehicle dynamics . . . . .	5
2.2	Discrete Kalman filter . . . . .	6
2.3	Extended Kalman filter . . . . .	7
<b>3</b>	<b>Estimator model</b>	<b>9</b>
3.1	Road slope estimator . . . . .	9
3.2	Mass estimator . . . . .	10
<b>4</b>	<b>Testing environments</b>	<b>13</b>
4.1	SimDriveline . . . . .	13
4.2	A simple car model . . . . .	13
4.3	Volvo V60: Off-line . . . . .	13
4.4	Volvo V60: On-line . . . . .	14
<b>5</b>	<b>Results and discussion</b>	<b>15</b>
5.1	Simulation results . . . . .	15
5.2	Test results . . . . .	16
5.2.1	Off-line mass estimation . . . . .	17
5.2.2	On-line mass estimation . . . . .	23

5.3	Filter sensitivity . . . . .	24
5.4	Future work . . . . .	26
<b>6</b>	<b>Conclusions</b>	<b>27</b>
	<b>Bibliography</b>	<b>29</b>



# List of parameters

$A_f$	largest cross-section of vehicle
$a$	accelerometer acceleration
$\alpha$	road slope
$C_d$	drag coefficient
$g$	gravitational acceleration
$K$	Kalman gain
$m$	vehicle mass
$\mu$	coefficient of rolling resistance
$P$	error covariance matrix
$P_p$	predicted error covariance matrix
$Q$	process disturbance covariance matrix
$R$	measurement disturbance covariance matrix
$r$	wheel radius
$\rho$	air density
$T$	torque acting on the wheels
$T_s$	sampling time
$u$	control signals
$v$	longitudinal speed of the vehicle
$v_w$	headwind speed
$x$	states
$\hat{x}$	estimated states
$\hat{x}_p$	predicted states



# Chapter 1

## Introduction

Automotive companies compete in delivering the best driving experience. One important factor is the performance feel, e.g. how the vehicle responds to the driver's commands. To be able to deliver the desired performance feel and improve drivability it is important to estimate certain parameter values more accurately. The mass of the vehicle and the road slope strongly affects how the vehicle behaves. In order to assure that the correct force is delivered, as demanded by the driver, it is important to estimate these two parameters.

### 1.1 Related work

Several vehicle mass and road slope estimation studies have been made. In these studies, trucks have mainly been studied since the total weight of such a vehicle can change dramatically depending on the type of load.

In *Adaptive Vehicle Weight Estimation* [1] the mass of a truck is estimated by measuring engine torque, as well as shaft and vehicle speed. The estimator is modelled such that multiple measurements form a linear equation, and from the tangential slope of this equation the mass is given. With the mass known, the road slope can be calculated. Estimation is done during both acceleration and gear shifting, with an accuracy of  $\pm 10\%$ .

A *study on road slope estimation for automatic transmission control* [2] compares two methods for road slope estimation. One method determines the slope by the difference between acceleration measured by an accelerometer and the derivative of the vehicle velocity. The other method relies on an engine torque estimation to determine the slope, but is paused during braking and gear shifting. The method using an accelerometer proved simpler and more accurate.

The same conclusion is drawn in *Road Slope and Vehicle Mass Estimation Using Kalman Filtering* [3] which uses an extended Kalman filter for mass estimation.

The advantages of using an accelerometer are also shown in *Vehicle Mass and Road Grade Estimation Using Kalman Filter* [4] which presents a method to estimate vehicle mass and road grade using an extended Kalman filter, with and without an accelerometer. The estimator is paused during gear shifting (as opposed to [1]), braking and for certain limits on speed and torque.

*Compression Braking Control for Heavy-Duty Vehicles* [5] uses an MRAC (Model Reference Adaptive Controller) for longitudinal speed control in heavy-duty vehicles by braking, which requires vehicle mass and road slope estimation. A control law is designed which finds the true mass and road grade within 45 s. If the parameters leave the regions which they are known to physically lie within, then the estimator is paused.

*Road Grade and Vehicle Parameter Estimation for Longitudinal Control Using GPS* [6] estimates the road slope, vehicle mass, rolling resistance and aerodynamic drag for a passenger car using GPS antennas. Two configurations are compared. The first configuration consists of a single antenna, where the vertical and horizontal speed ratio is compared to find the slope. The second configuration obtains the slope using two antennas with fixed positions by measuring their relative displacement. Other measurements required for the mass estimation include engine propulsion force, vehicle acceleration and vehicle speed. Turning, braking and wheel slip is not taken into consideration. Using a single equation relating the measurements and the unknown parameters, together with lots of measurement points and an unspecified recursive algorithm, the mass, rolling resistance and aerodynamic drag can be determined. The result is that the estimated mass converges to within 2% of the true value in 12 s.

## 1.2 Purpose

The purpose of this thesis is to develop a model in MATLAB/Simulink which estimates a vehicle's mass. In order to accurately calculate the mass, the road slope also needs to be estimated. The mass estimator should be implemented and tested in a real vehicle; therefore it is desired to be as robust as possible.

## 1.3 Objectives

The estimated mass should be within 5% of the true mass, in less than five minutes of driving.

## 1.4 Method

The available signals are the vehicle's measured speed, acceleration, proper acceleration (as measured by a longitudinal accelerometer) and the wheel torque.

With the use of the accelerometer the road slope is estimated. When the slope is known the mass can be derived from Newton's second law using the wheel torque, acceleration, rolling resistance and aerodynamic drag. A Kalman filter is used for mass estimation and to reduce the influence of disturbances.

The estimator is tested in simulation environments and on real data, collected from several driving sessions with a Volvo V60 with an automatic gearbox.

## 1.5 Delimitations

The scope of the thesis is to estimate vehicle mass and road slope, not how these can be used to improve drivability.

The model is created for use in passenger cars, not heavy vehicles, under normal driving conditions (e.g. not off-road), possibly with a trailer or caravan.

The following simplifications and assumptions are made:

- The true mass is assumed to lie between 1800 and 5000 kg.
- Estimation of the slope only considers longitudinal slopes of max  $\pm 35\%$  ( $\approx 20^\circ$ ). The estimator will not be tested for steeper slopes.
- The change in pitch of the vehicle at certain driving situations or with uneven load distributions is not considered separately, but is part of the road slope estimation.
- Wheel slip is assumed to be negligible.
- The effects of lateral forces are neglected.

## 1.6 Report outline

In *chapter 2*, the theory necessary to understand the estimation algorithm is presented. *Chapter 3* motivates and presents the choice of estimator algorithm. The testing environments are described in *chapter 4* and results from the tests are shown and discussed in *chapter 5*. Finally, in *chapter 6*, the main conclusions are presented.



# Chapter 2

## Background theory

This chapter gives an overview of the vehicle dynamics used in the simulation environment and the theory behind the mass estimating Kalman filter.

### 2.1 Vehicle dynamics

A moving vehicle is subject to several forces, as seen in figure 2.1. The longitudinal equation of motion becomes:

$$m\dot{v} = F_{traction} - F_{air} - F_{\mu} - F_g \quad (2.1)$$

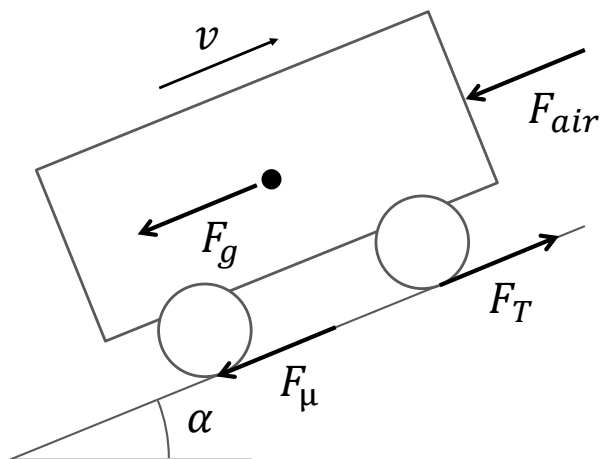


**Figure 2.1:** Forces acting on a vehicle.

The *traction force*  $F_{traction}$  is the propulsive force of the vehicle, which depends on the torque acting on the wheels  $T$  and the wheel radius  $r$ :

$$F_{traction} = \frac{T}{r} \quad (2.2)$$

The *air resistance*  $F_{air}$  depends on the density of the air  $\rho$ , the headwind speed  $v_w$  and the aerodynamic properties of the vehicle  $C_d$ , as well as its longitudinal speed  $v$  and its largest cross-section  $A_f$ :

$$F_{air} = \frac{1}{2}\rho C_d A_f (v + v_w)^2 \quad (2.3)$$

Another force acting against the direction of movement is the *rolling resistance*  $F_\mu$ , which is due to friction and the deformation of the wheels. It depends on the coefficient of rolling resistance  $\mu$ , the road slope  $\alpha$ , the vehicle mass  $m$  and the gravitational acceleration  $g$ :

$$F_\mu = \mu m g \cos \alpha \quad (2.4)$$

The deformation generally increases with the speed, but only significantly for speeds well over common speed limits [7]. Therefore  $\mu$  is assumed to be speed independent.

In addition to these forces, the *gravitational pull*  $F_g$  can act as either an accelerating or decelerating force, depending on the road slope. Vehicle mass, road slope and the gravitational acceleration determines the magnitude of the force:

$$F_g = m g \sin \alpha \quad (2.5)$$

General reference: *Bosch Automotive Handbook* [8].

## 2.2 Discrete Kalman filter

The discrete Kalman filter estimates the states of a linear system described by the difference equation

$$x(k) = Ax(k-1) + Bu(k-1) + w(k-1) \quad (2.6)$$



by treating it as an optimization problem, solved by minimizing the estimator error covariance  $P$ . Available measurements of states are given by

$$z(k) = Hx(k) + v(k) \quad (2.7)$$

where the process disturbance  $w \sim N(0, Q)$  is normally distributed white noise, with zero mean and variance  $Q$ , and the measurement disturbance  $v \sim N(0, R)$  is normally distributed white noise with zero mean and variance  $R$ .

The Kalman filter makes predictions of the states based on previous estimated states and control signals. Then it calculates an observer gain  $K$  based on properties of the system and process disturbances. The estimates are calculated by weighing predicted states and measured states against each other, such that it minimizes  $P$  [9].

Since only the estimates of the states can be determined,  $x$  will henceforth be approximated with the estimated states  $\hat{x}$ .

The procedure of the Kalman filter for one sample [10]:

1. Predict states:

$$\hat{x}_p(k) = A\hat{x}(k-1) + Bu(k-1) \quad (2.8)$$

2. Predict error covariance:

$$P_p(k) = AP(k-1)A^\top + Q \quad (2.9)$$

3. Compute the Kalman gain:

$$K(k) = P_p(k)H^\top (HP_p(k)H^\top + R)^{-1} \quad (2.10)$$

4. Estimate the states by correcting the predictions with measurements:

$$\hat{x}(k) = \hat{x}_p(k) + K(k)(z(k) - H\hat{x}_p(k)) \quad (2.11)$$

5. Update the error covariance:

$$P(k) = (I - K(k)H)P_p(k) \quad (2.12)$$

## 2.3 Extended Kalman filter

The regular Kalman filter works well for linear processes, but has to be modified when used for nonlinear processes. In such cases the Kalman filter has to be

linearized around the estimated states at every sample, thus becoming an extended Kalman filter (EKF).

The process can more generally be described by the nonlinear difference equation

$$x(k) = f(x(k-1), u(k-1), w(k-1)) \quad (2.13)$$

with measurements

$$z(k) = h(x(k), v(k)) \quad (2.14)$$

and with disturbances  $w \sim N(0, Q)$  and  $v \sim N(0, R)$  as before.

The main difference between the EKF and the standard Kalman filter is the required linearization of the nonlinear system equation. Since the values of  $w$  and  $v$  are unknown at each time step, an approximation is to linearize around  $w = 0, v = 0$ .

The procedure of the EKF for one sample [10]:

1. Predict states:

$$\hat{x}_p(k) = f(\hat{x}(k-1), u(k-1), 0) \quad (2.15)$$

2. Linearize:

$$A_{[i,j]} = \frac{\partial f_i}{\partial x_j}(\hat{x}(k-1), u(k-1), 0) \quad (2.16)$$

$$W_{[i,j]} = \frac{\partial f_i}{\partial w_j}(\hat{x}(k-1), u(k-1), 0) \quad (2.17)$$

$$H_{[i,j]} = \frac{\partial h_i}{\partial x_j}(\hat{x}_p(k), 0) \quad (2.18)$$

$$V_{[i,j]} = \frac{\partial h_i}{\partial v_j}(\hat{x}_p(k), 0) \quad (2.19)$$

3. Predict error covariance:

$$P_p(k) = A(k)P(k-1)A^\top(k) + W(k)Q(k-1)W^\top(k) \quad (2.20)$$

4. Compute the Kalman gain:

$$K(k) = P_p(k)H^\top(k)(H(k)P_p(k)H^\top(k) + V(k)R(k)V^\top(k))^{-1} \quad (2.21)$$

5. Estimate the states by correcting the predictions with measurements:

$$\hat{x}(k) = \hat{x}_p(k) + K(k)(z(k) - h(\hat{x}_p(k), 0)) \quad (2.22)$$

6. Update the error covariance:

$$P(k) = (I - K(k)H(k))P_p(k) \quad (2.23)$$

# Chapter 3

## Estimator model

Out of the two methods for road slope estimation suggested by [2] the use of an accelerometer is the most advantageous. Since an accelerometer is available in the Volvo V60, there is no extra cost associated with it. The use of an accelerometer is further supported by [3].

The drive torque directly at the wheels is accessible; therefore no modelling of the driveline is required. Since the estimation is mainly done for the Volvo V60, which has an automatic gearbox, estimation during gear shifting as in [1] is not possible. The extended Kalman filter presented in [3] seems suitable in theory, and is shown to be so when put into practice in [4]. The MRAC suggested by [5] also seems feasible; it was however only tested in a simulation environment.

Although [6] was one of the few projects which was designed for and implemented in a passenger car instead of a truck, the use of antennas to estimate the road slope is not feasible in and beyond the scope of this thesis. The mass estimation was only tested for straight driving, but is fast and accurate.

The EKF is a filter widely used for estimation and has performed well in previous studies. Therefore it was chosen as the mass estimator. In this chapter, the design of the estimator is explained.

### 3.1 Road slope estimator

An accelerometer measures proper acceleration. This means that if the vehicle is standing still on a slope then the amount of gravitational acceleration acting on the car can be measured and the slope calculated. Since the acceleration of the vehicle also is measured, the difference between the two accelerations determines the road slope also when moving, as follows:

$$\alpha = \arcsin \frac{a - \dot{v}}{g} \quad (3.1)$$

### 3.2 Mass estimator

Combining the vehicle dynamic equations (2.1) - (2.5) results in the following continuous equation:

$$\dot{v} = \frac{T}{rm} - \frac{1}{2m}\rho C_d A_f (v + v_w)^2 - \mu g \cos \alpha - g \sin \alpha \quad (3.2)$$

With this equation describing the system, the states are chosen as  $x_1 = v$ ,  $x_2 = 1/m$ ,  $x_3 = \alpha$  and the control signal as  $u = T$ . Since  $m$  is constant  $x_2$  could be considered a slowly varying parameter with a small disturbance  $w_m$ .  $x_3$  is also modelled as an unknown parameter with disturbance  $w_\alpha$ .

The choice of  $x_2 = 1/m$  instead of  $x_2 = m$  simplifies the linearization of the Kalman filter. This also turned out to give a faster filter which was less sensitive to the choice of initial mass.

With process disturbances  $w_1 = w_T$ ,  $w_2 = v_w$ ,  $w_3 = w_m$ ,  $w_4 = w_\alpha$  added, the state space equations become:

$$\dot{x}_1 = f_1 = \frac{(u + w_1)x_2}{r} - \frac{x_2}{2}\rho C_d A_f (x_1 + w_2)^2 - \mu g \cos x_3 - g \sin x_3 \quad (3.3)$$

$$\dot{x}_2 = f_2 = w_3 \quad (3.4)$$

$$\dot{x}_3 = f_3 = w_4 \quad (3.5)$$

In order to implement the model it must be discrete. Discretization was done using the forward Euler method, which approximates the continuous differential equation

$$\dot{x} = f(t, x(t))$$

with a difference equation

$$x(k+1) = x(k) + T_s f(kT_s, x(kT_s))$$

where  $T_s$  is the step time.

Discretizing with a step time  $T_s$  results in the system equations

$$\hat{x}_1(k+1) = \hat{x}_1(k) + T_s \left( \frac{(u(k) + w_1(k))\hat{x}_2(k)}{r} + \right. \\ \left. - \frac{\hat{x}_2(k)}{2}\rho C_d A_f (\hat{x}_1(k) + w_2(k))^2 - \mu g \cos \hat{x}_3(k) - g \sin \hat{x}_3(k) \right) \quad (3.6)$$

$$\hat{x}_2(k+1) = \hat{x}_2(k) + T_s w_3(k) \quad (3.7)$$

$$\hat{x}_3(k+1) = \hat{x}_3(k) + T_s w_4(k) \quad (3.8)$$

with measurements:

$$z(k) = Hx(k) + Vv(k) = \begin{bmatrix} 1 & 0 & 0 \\ 0 & 0 & 1 \end{bmatrix} \hat{x}(k) + \begin{bmatrix} 1 & 0 \\ 0 & 1 \end{bmatrix} v_k \quad (3.9)$$

To linearize around the latest estimate  $\hat{x}(k-1)$ , the matrices  $A$  and  $W$  have to be recalculated at each time step:

$$A = \begin{bmatrix} \frac{\partial f_1}{\partial x_1} & \cdots & \frac{\partial f_1}{\partial x_3} \\ \vdots & \ddots & \vdots \\ \frac{\partial f_3}{\partial x_1} & \cdots & \frac{\partial f_3}{\partial x_3} \end{bmatrix} = \begin{bmatrix} A_1 & A_2 & A_3 \\ 0 & 1 & 0 \\ 0 & 0 & 1 \end{bmatrix}$$

$$A_1 = 1 - T_s \rho C_d A_f \hat{x}_1(k-1) \hat{x}_2(k-1)$$

$$A_2 = T_s \left( \frac{u(k-1)}{r} - \frac{\rho C_d A_f \hat{x}_1^2(k-1)}{2} \right)$$

$$A_3 = T_s g (\mu \sin \hat{x}_3(k-1) - \cos \hat{x}_3(k-1))$$

$$W = \begin{bmatrix} \frac{\partial f_1}{\partial w_1} & \cdots & \frac{\partial f_1}{\partial w_4} \\ \vdots & \ddots & \vdots \\ \frac{\partial f_3}{\partial w_1} & \cdots & \frac{\partial f_3}{\partial w_4} \end{bmatrix} = \begin{bmatrix} W_1 & W_2 & 0 & 0 \\ 0 & 0 & T_s & 0 \\ 0 & 0 & 0 & T_s \end{bmatrix}$$

$$W_1 = -T_s \rho C_d A_f \hat{x}_1(k-1) \hat{x}_2(k-1)$$

$$W_2 = \frac{T_s \hat{x}_2(k-1)}{r}$$

Since (3.9) is already linear there is no need to linearize  $H$  nor  $V$ .

## On/off logics

The torque measurements are not accurate when braking, which will result in large errors in the mass estimation. Since it is enough to know when the vehicle is braking, the estimation algorithm is paused when the estimated brake force is not zero, in order to avoid this problem.

To pause the algorithm, the states  $\hat{x}$  and the error covariance matrix  $P$  are held constant. In other words, the states will not be updated as long as the vehicle is braking and the internal parameters of the filter will not change. Note that this applies for all states, but this is not an issue since the only interesting output from

the filter is the mass. The measurements of the other two states are considered trustworthy.

# Chapter 4

## Testing environments

This chapter describes the various simulation environments that were used to test and tune the estimator.

### 4.1 SimDriveline

SimDriveline is a Simscape based library in the Simulink environment that models and simulates drivetrain systems. The full drivetrain model called *sdLvehicle* was used to initially test the behaviour of the Kalman filter for simple driving scenarios. However, this model did not fulfill all the requirements, so a new, simple car model was created.

### 4.2 A simple car model

The simple car model that was created was based on exactly the same physics as the Kalman filter. The vehicle model used wheel torque and road profile as input. The wheel torque was provided by a "driver block", which basically was a simple PI-regulator following a reference speed graph. See figure 4.1 for an overview of the system. The model was mainly used to see how the filter handled disturbances, such as wind and measurement noise, and the filter was tuned accordingly.

### 4.3 Volvo V60: Off-line

To properly test the estimator, real data was collected in several driving scenarios. A computer was connected to a Volvo V60 and the interesting signals were logged with INCA software. All signals were re-sampled at 100 Hz when imported into MATLAB.

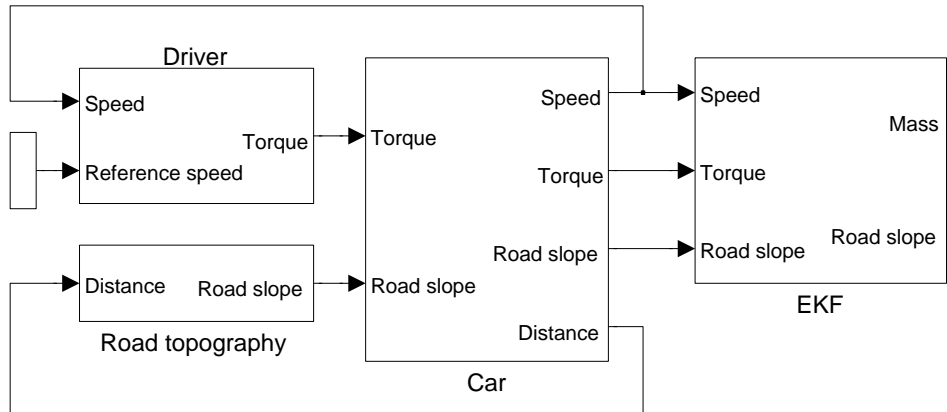


**Figure 4.1:** Schematic overview of the Simulink model.

The data collection was performed on different roads and with different loads. The estimator was tested on the following roads:

*Torslanda 1:* Short, flat test track.

*Torslanda 2:* Long route with varying road slope (public road).

*Test track 1:* Flat test track considerably bigger than Torslanda 1.

*Test track 2:* A typical country road with varying road slope.

*Test track 3:* Gravel road with varying road slope.

## 4.4 Volvo V60: On-line

To implement the mass estimator, the Simulink model was converted using TargetLink. Code was generated and downloaded into the V60.

At the end of the project a series of tests were made to ensure that the estimator gives similar result in the car as in the simulation environment.



# Chapter 5

## Results and discussion

In this chapter, the behaviour of the mass estimation filter is presented and discussed. This is done for both simulated and collected data. Finally, sources of error and possible future improvements are discussed.

### 5.1 Simulation results

In this section, results based on simulated input data are presented. The vehicle model followed a simple reference speed graph (see figure 5.1b) on a road with realistic slope (figure 5.1d). Based on the speed, road slope and wheel torque (figure 5.1c) the filter estimated the mass (figure 5.1a). Note that the on/off-logic was not used in the simulated environment.

The test shows that the filter is fast and accurate; the estimated mass lies well within 5% of the true mass after a few seconds. The road slope estimation follows the true slope rather well.

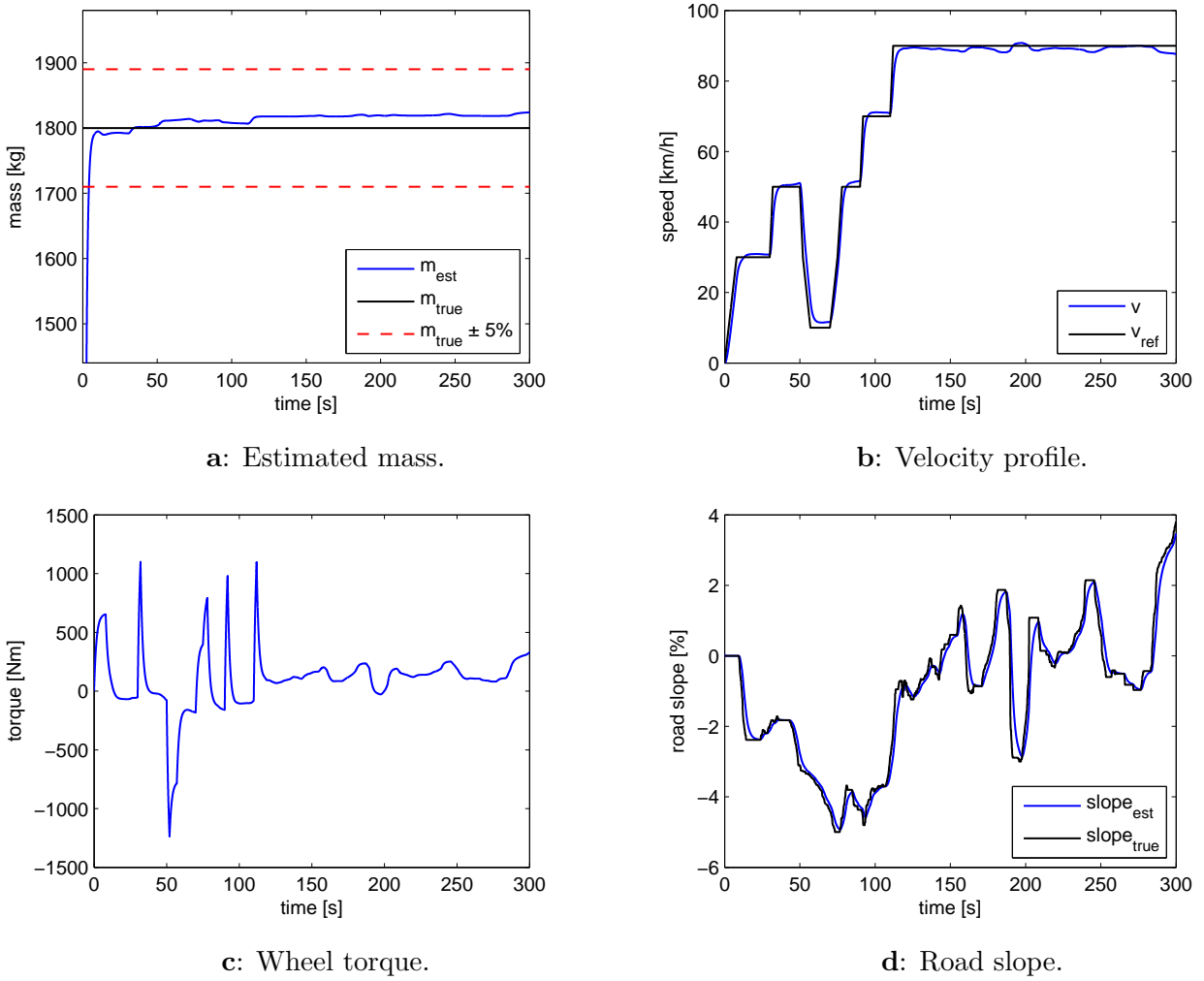


**Figure 5.1:** Inputs and outputs of the filter for the *Simple car model*.

## 5.2 Test results

Results based on real input data are presented in this section. The off-line estimations are made in Simulink and the on-line estimations are results from the estimation algorithm running in real time in a Volvo V60.

### 5.2.1 Off-line mass estimation

Mass estimation results for the more interesting driving scenarios are presented below. Data for different velocities, inclinations and loads were collected in order to test the performance and robustness of the filter in a variety of environments.

#### Torslanda 1 and 2

Initially, data was collected on *Torslanda 1*, which is a short and flat test track, by driving several laps. The advantage of testing on a flat track is that the road slope is close to zero, which makes it easier to determine possible sources of error. The other test route, *Torslanda 2*, is a public road with varying road slope, different speed limits and natural start-stop situations. This test represents a normal driving scenario. Both these test drives were performed with a Volvo V60 carrying three persons.

Mass estimation results, and the signals used in the estimation algorithm, are presented in figure 5.2 and figure 5.3. The road slope is calculated from accelerometer measurements, while the torque and the velocity are directly available as measurements.

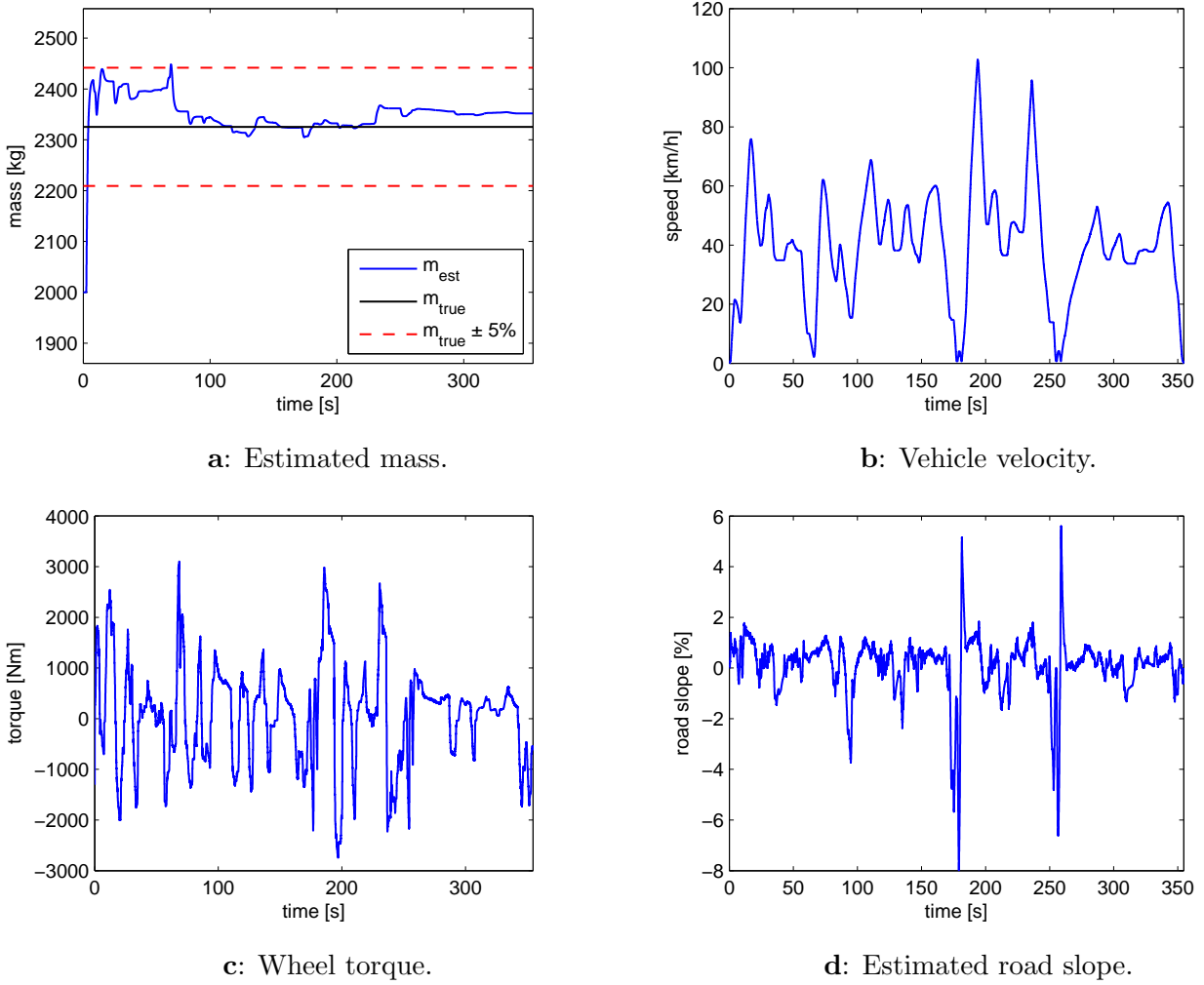


**Figure 5.2:** Inputs and outputs of the filter for the test on *Torslanda 1*.

<i>Mean velocity [km/h]</i>	<i>Active estimation [%]</i>
39.9	0.686

**Table 5.1:** Additional data for *Torslanda 1*.

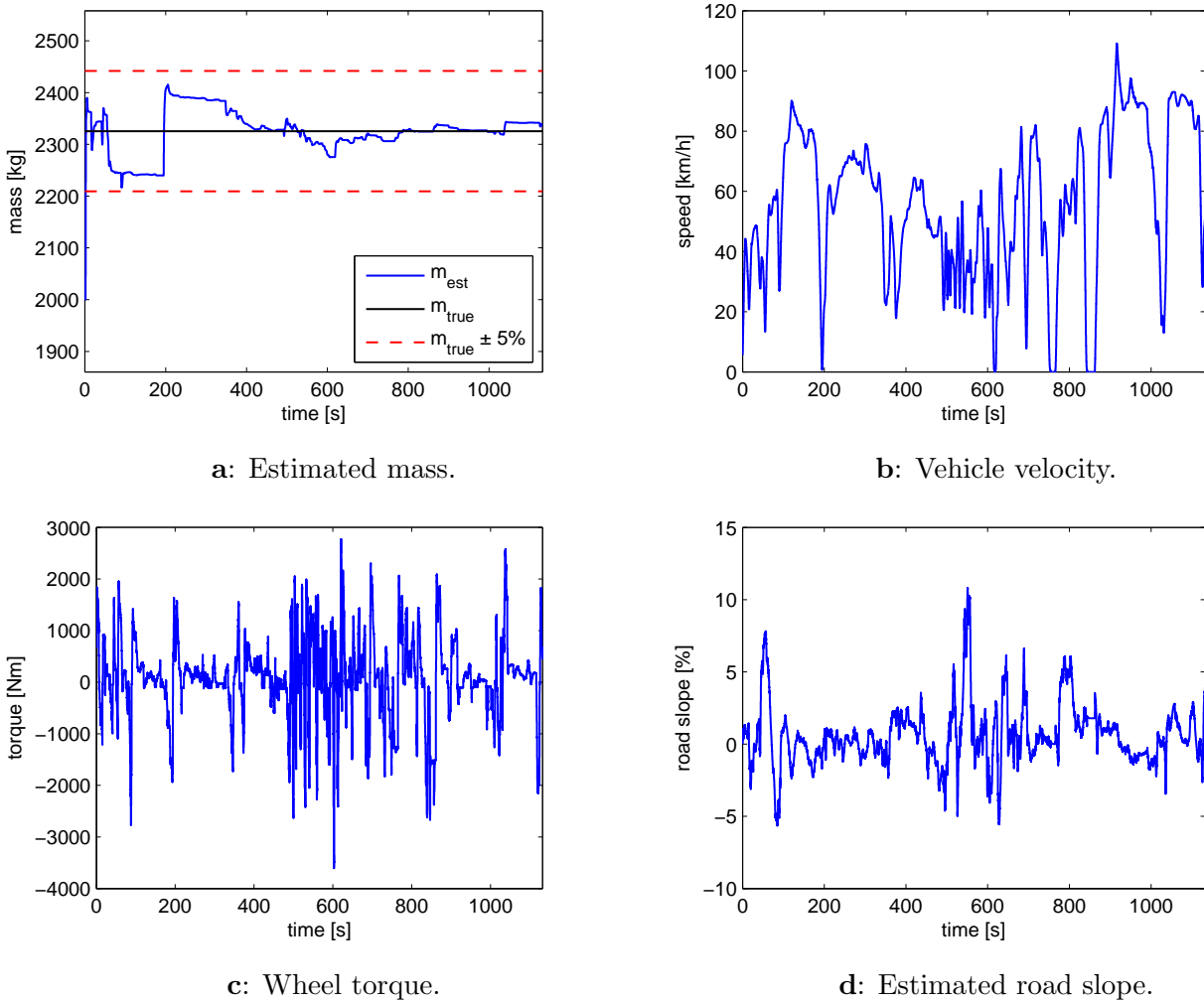


**Figure 5.3:** Inputs and outputs of the filter for the test on *Torslanda 2*.

<i>Mean velocity [km/h]</i>	<i>Active estimation [%]</i>
55.8	0.776

**Table 5.2:** Additional data for *Torslanda 2*.

The signals in figure 5.2b-d are the signals that are used by the EKF to estimate the vehicle mass, seen in figure 5.2a.

The estimated mass quickly settles within the desired 5% limits. It is not as accurate as the simulation result shown earlier (figure 5.1a), but roughly as fast. The real car is subject to more disturbances than the simulated car, such as a

more uneven road surface and wind from different directions. In addition, the brake torque measurement is not as accurate as in the simulated version; therefore the on/off-logics are used. The performance in this test is more than acceptable.

As can be seen in the road slope plot (figure 5.2d), the track is probably not completely flat. The estimated road slope is varying between -2% and +2%. This is most likely a combination of small road grade variations, an uneven road surface and changes in the vehicle pitch angle. The large changes in road slope at approximately 180 and 260 seconds occur while braking, stopping and reversing the vehicle. The on/off-logics counter this effect such that it does not affect the mass estimation noteworthy.

Figure 5.3 shows the corresponding results and signals for the test on a public road, *Torslanda 2*. The mean velocity is higher than in the previous case, the estimation algorithm is active for a higher percentage of the time (see tables 5.1 and 5.2) and the road slope is varying. The estimated mass plot is not as smooth as in figure 5.2, but still accurate and fast enough. The difference is likely due to more distinct accelerations on the test track than on the public road.

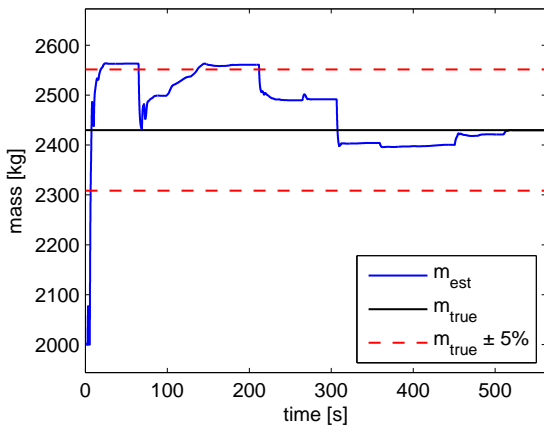
Since there is no true road slope to compare the estimated slope with, and it is considered accurate enough for the mass estimation algorithm, it is not very interesting when analysing the mass estimation. The wheel torque is related to the propulsion of the vehicle, i.e. accelerations and countering outer forces acting on the vehicle, but is not necessary to understand the performed tests. These signals will therefore not be shown in following cases. The vehicle velocity is interesting because it is closely related to the air resistance, and because it gives a picture of how the test was carried out.

### Test track 1, 2 and 3

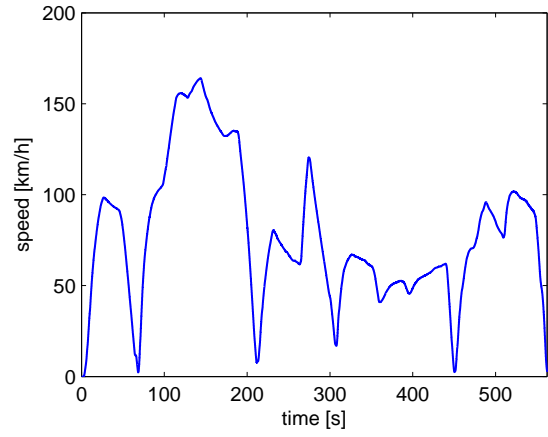
In order to further test the filter, additional tests were performed. Results from the combinations of three different test tracks and two different kinds of load are presented in this section.

In the first three cases (shown in figure 5.4) the car was loaded with 200 kg of extra weight and was carrying two persons. In the next three cases (figure 5.5) the extra weight was removed and a caravan weighing 1300 kg attached. The tests with a caravan were performed to observe how the estimation algorithm behaves when the factors  $C_d$  and  $A_f$  in equation (2.3) deviates from the filter model.

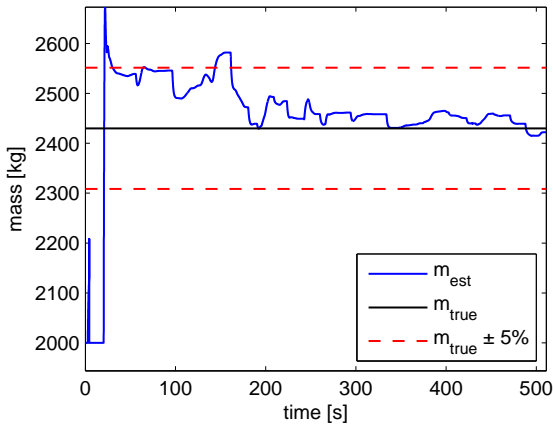
Figure 5.4 and figure 5.5 show mass estimation results and measured velocities for the flat road of *Test track 1* (subfigures a and b), the varying country road in *Test track 2* (subfigures c and d) and the gravel road of *Test track 3* (subfigures e and f).



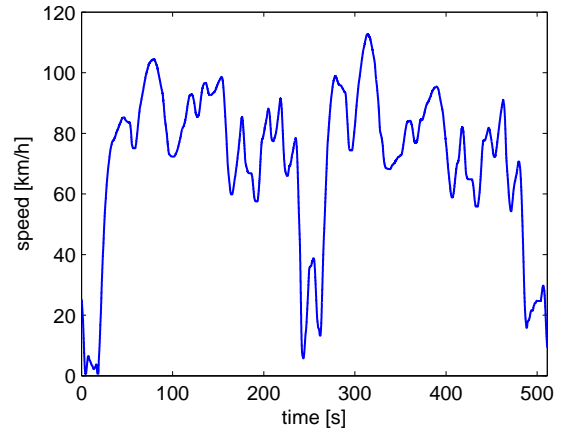
a: Estimated mass, *Test track 1*.



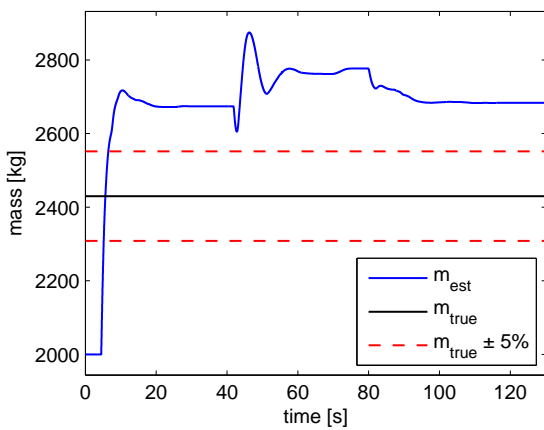
b: Vehicle velocity, *Test track 1*.



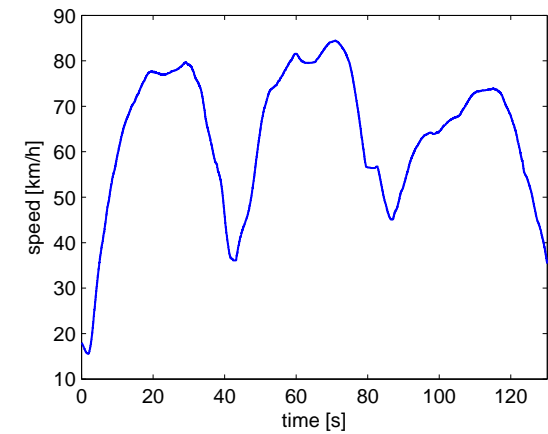
c: Estimated mass, *Test track 2*.



d: Vehicle velocity, *Test track 2*.

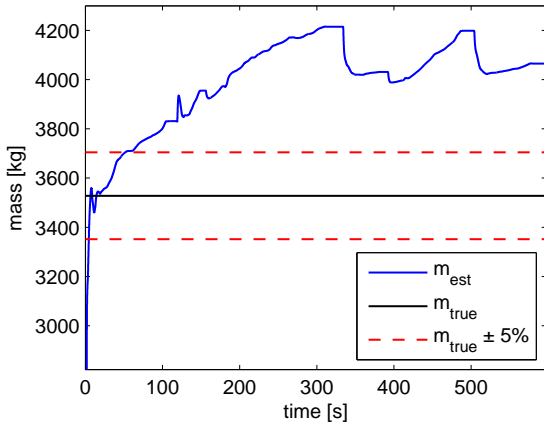


e: Estimated mass, *Test track 3*.

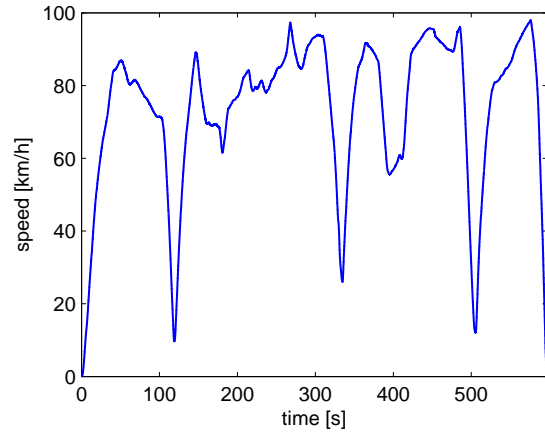


f: Vehicle velocity, *Test track 3*.

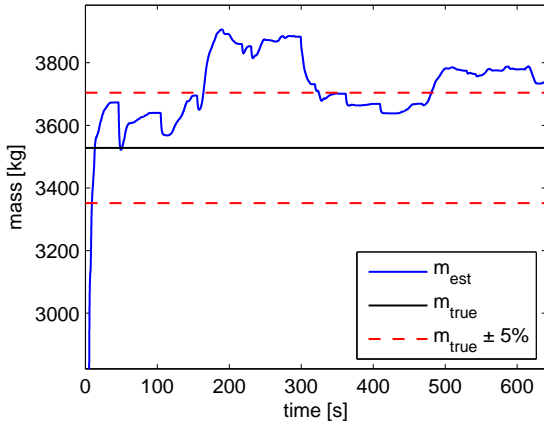
**Figure 5.4:** Estimated masses and vehicle velocities on different test tracks, *without* a caravan.



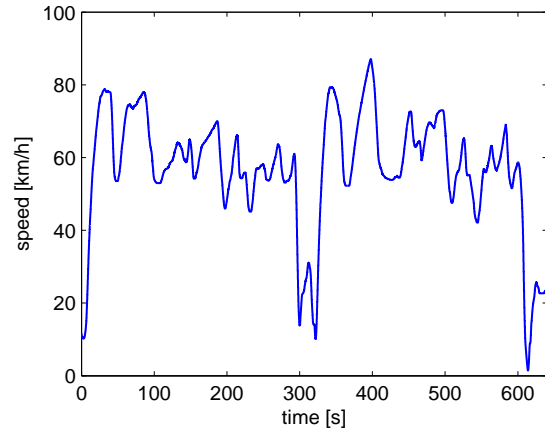
a: Estimated mass, *Test track 1*.



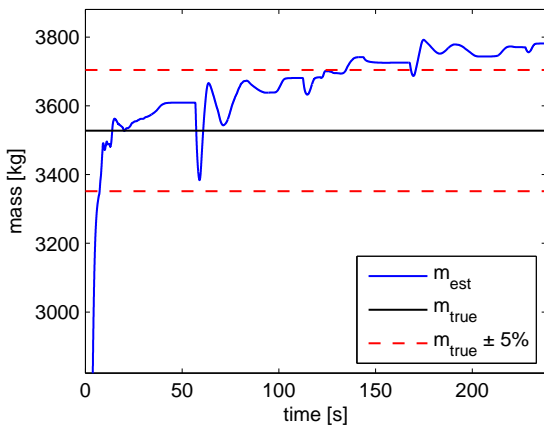
b: Vehicle velocity, *Test track 1*.



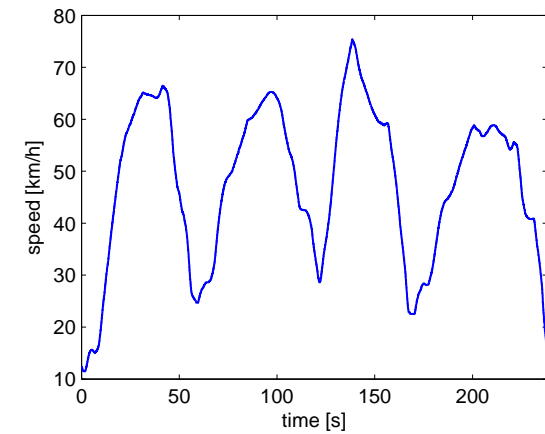
c: Estimated mass, *Test track 2*.



d: Vehicle velocity, *Test track 2*.



e: Estimated mass, *Test track 3*.



f: Vehicle velocity, *Test track 3*.

**Figure 5.5:** Estimated masses and vehicle velocities on different test tracks, *with a caravan*.



Figure 5.4 shows that the mass estimation is working as intended on the asphalt roads (subfigures a and c) but settles on a value outside the 5% margins for the gravel road data (subfigure e). Even though this test is for a smaller time interval, it does not show the same tendencies to approach the true mass as the other cases. The reason for the behaviour on the gravel road is due to a higher rolling resistance coefficient, which is dependent on the road surface. The effects of changes in the rolling resistance coefficient are discussed in section 5.3.

Note that the effects of the on/off-logics clearly can be seen in figure 5.4a where the mass is held constant for longer periods than in the other cases, resulting in flat sections in the graph.

The estimator is not accurate enough for any of the caravan cases, as can be seen in figure 5.5. This is because the caravan changes the vehicle's aerodynamical properties,  $C_d A_f$ . In figure 5.5a it is clear that the high velocities together with the changed aerodynamical parameters result in large estimation errors. However, the estimation is initially very accurate while the velocity is still low. This is because the aerodynamic drag depends on the square of the velocity. This issue is further discussed in section 5.3. A similar behaviour is shown in figure 5.5c, but since the velocities generally are lower the error is not as large. The velocities for the test on the gravel road (figure 5.5e) are even lower, but the rolling coefficient is higher, resulting in estimation errors outside the set margins, but in an unexpected way. Generally a higher rolling resistance results in much larger initial errors than seen in the figure.

### 5.2.2 On-line mass estimation

The estimator showed the same behaviour when tested in real-time in a car as in the off-line estimations. This shows that the code generating stage went as intended and that this does not provide an obstacle for implementing the model in a car.

### 5.3 Filter sensitivity

To show the influences of errors in  $\mu$  and  $C_d A_f$ , the collected data from *Torslanda 1* is reused in additional mass estimations with these parameters changed. Factors  $k_\mu$  and  $k_{C_d A_f}$  were added to  $\mu$  and  $C_d A_f$  to show how these parameters were changed. A k-value of 1 naturally corresponds to the original parameter value. The resulting mass can be seen in figure 5.6 for different values of  $k_\mu$  and in figure 5.7 for different values of  $k_{C_d A_f}$ .

$k_\mu < 1$  corresponds to driving on a rougher surface than what the filter is designed for, i.e. rougher than asphalt, such as gravel road.  $k_\mu > 1$  corresponds to driving on a very smooth surface with special tyres.

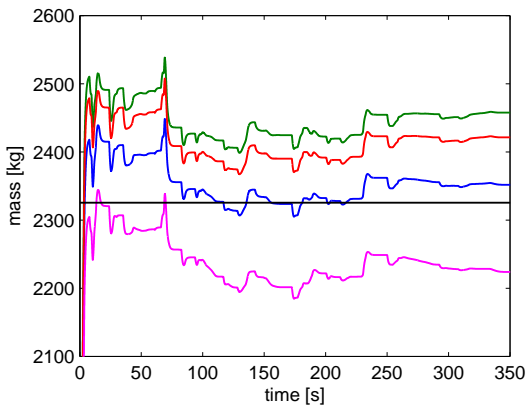
$k_{C_d A_f} < 1$  means that the aerodynamic properties are worse than expected, e.g. due to an attached caravan or similar. In the same sense a  $k_{C_d A_f} > 1$  means that the aerodynamics are better, which is highly unlikely but still shown for illustrative purposes.

As seen in figure 5.6b the mass deviation is immediately evident for changes in  $k_\mu$ , while in figure 5.7b the mass does not deviate immediately. This is due to that an error in  $C_d A_f$  only noticeably affects the air resistance for higher velocities, due to the squared velocity dependency.

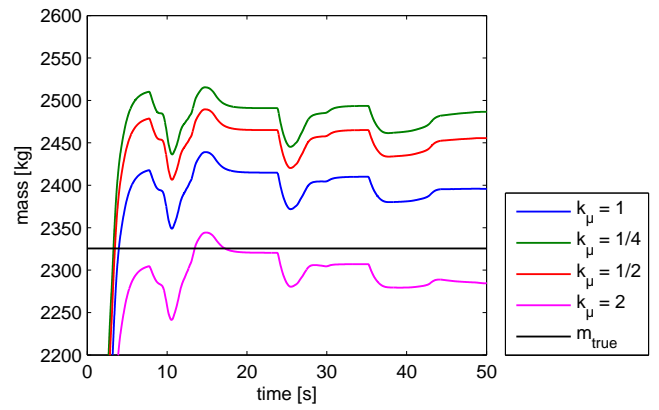
Since the changes are made in the filter parameters and not in the test environment (the car or the road), only the general behaviour of such parameter errors are shown. The errors shown will therefore not be of the same size as they would have been if the rolling resistance coefficient of the road or the aerodynamical properties of the vehicle were changed. Using the same data and changing the filter parameters makes the results directly comparable.

Since the wind influences the air resistance equation (2.3) as much as the vehicle velocity does, it can easily affect the estimation. It is however hard to take this into account since it can change rapidly and is difficult to measure.

Due to simplifications in the filter model, influences by lateral forces and the wheel slip are neglected. However, these are generally not considered to affect the mass estimation to any large extent.

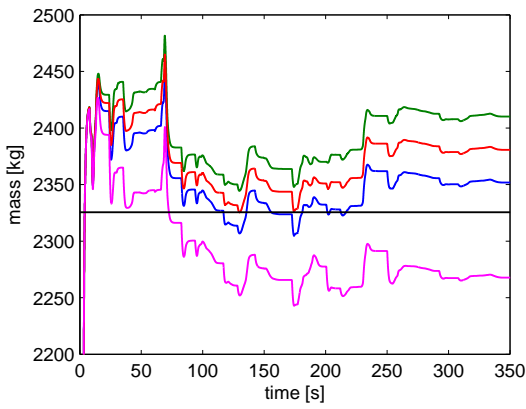


a: Changed  $k_\mu$ , overview.

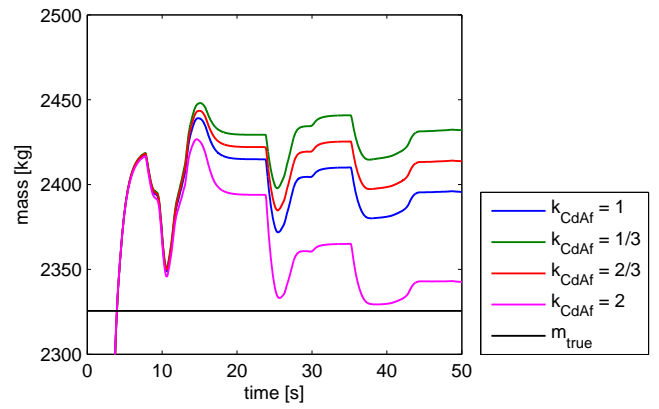


b: Changed  $k_\mu$ , first 50 s.

**Figure 5.6:** Estimated mass for different rolling resistance values.



c: Changed  $k_{C_dA_f}$ , overview.



d: Changed  $k_{C_dA_f}$ , first 50 s.

**Figure 5.7:** Estimated mass for different aerodynamical property values.

## Sources of error

The following will, or are likely to, cause an erroneous mass estimation.

**Aerodynamics:** Caravans, trailers, roof boxes or even open windows will change the aerodynamics of the vehicle.

**Lateral forces:** The lateral forces occurring due to steering has not been taken into account.

**Rolling resistance:** Dependent upon road surface, tyres and vehicle speed, although the speed is considered a minor issue at normal velocities.

**Wheel slip:** As with the lateral forces it is considered negligible but could potentially change the results slightly.

**Wind:** Can change rapidly, is therefore difficult to model.

## 5.4 Future work

As seen in the tests with a caravan and in the sensitivity analysis, errors in the filter parameters can lead to large mass estimation errors.  $C_d$ ,  $A_f$  and  $\mu$  are parameters that are likely to vary in day-to-day usage, it would therefore be desirable to allow for these changes and estimate these parameters for improved mass estimation. The wind speed will probably be a problem when trying to estimate the aerodynamical parameters. Instead of a separate  $C_d A_f$  estimation, where the wind speed would be a problem, the wind speed disturbances could be accounted for in an estimation of the entire air resistance  $F_{air}$ .

The influence of lateral forces and wheel slip could also be included in an estimator model. However, previous research in the area shows that the effects are negligible.

# Chapter 6

## Conclusions

The mass estimation algorithm works very well in cases when the aerodynamic parameters are known and the rolling resistance coefficient in the filter corresponds to the road surface. The filter is particularly good in driving scenarios with several, more distinct accelerations, such as in the test performed on *Torslanda 1* (figure 5.2). There is some room for deviations in the filter parameters since the estimated mass lies well within the 5% limit in most tests. Adding a caravan is an example of something which makes the estimated mass go outside the margins, since the aerodynamics of the complete vehicle are greatly affected.

The initial goal of getting an estimation that settles within 5% of the true mass in less than 5 minutes of driving is easily achieved; it is often reached within seconds.

Even though several tests were made, the filter does not always behave as expected (see figure 5.5e). If this mass estimation algorithm is to be used in a passenger car, which was part of the initial objective, further testing and tuning is required. The main desired improvement to the filter is to increase its robustness by making it more adaptable to changes in  $\mu$  and  $C_d A_f$ . It would also be advantageous to implement an algorithm which decides when the estimation is "good enough" and then stops the estimation.



# Bibliography

- [1] Ritzén E. *Adaptive Vehicle Weight Estimation* [Master's Thesis]. Linköping University; 1998.
- [2] Ohnishi H, Ishii J, Kayano M, Katayama H. *A study on road slope estimation for automatic transmission control*. JSAE Review. 2000;21(2):235–240.
- [3] Lingman P, Schmidtbauer B. *Road Slope and Vehicle Mass Estimation Using Kalman Filtering*. Vehicle System Dynamics. 2002;37(Suppl.):12–23.
- [4] Jonsson Holm E. *Vehicle Mass and Road Grade Estimation Using Kalman Filter* [Master's Thesis]. Linköping University; 2011.
- [5] Druzhinina M, Moklegaard L, Stefanopoulou AG. *Compression Braking Control for Heavy-Duty Vehicles*. In: Proceedings of the American Control Conference. vol. 4; 2000. p. 2543–2547.
- [6] Bae HS, Ryu J, Gerdes JC. *Road Grade and Vehicle Parameter Estimation for Longitudinal Control Using GPS*. In: IEEE Conference on Intelligent Transportation Systems, Proceedings, ITSC; 2001. p. 166–171.
- [7] Genta G. *Motor Vehicle Dynamics*. World Scientific Publishing; 2006.
- [8] Bauer H. *Bosch Automotive Handbook*. 6th ed. Robert Bosch; 2004.
- [9] Åström KJ, Wittenmark B. *Computer-Controlled Systems*. 3rd ed. Prentice Hall; 1997.
- [10] Welch G, Bishop G. *An Introduction to the Kalman Filter*. University of North Carolina at Chapel Hill: Department of Computer Science; 2006.